SMOS+STORM Evolution

Blend High Wind Speed Database-
-User Manual-

Deliverable: BHWS-DATA-UM

Customer	ESA/ESRIN
ESA Contract Change Notice No	4000105171/12/I-BG
Document Reference	SMOSpluSTORM_EVOLU_BHWS_UDM_v1.0
Version/Rev	1.0
Date of Issue	28 Sept. 2017

	Function	Name	Signature	Date
Prepared by/Lead Author	Project Manager & Consortium	Fabrice Collard, Joseph Tenerelli, OceanDataLab		28 Sept. 2017
Accepted by	ESA technical Officer	Craig Donlon		

Table of Content

Summary

This User Manual document (BHWS-UM) relates to ESA contract CCN 4000105171/12/I-BG. This STSE project has one overall aim which is to ***Demonstrate the performance, utility and impact of SMOS L-band measurements at high wind speeds over the ocean during Tropical and Extra-Tropical storm conditions.***

Measurements of surface wind speed within Tropical and Extra Tropical storms are essential to the successful prediction of storm intensity and storm tracks with obvious societal benefits. Satellite measurements over the ocean surface derived from active microwave radars (scatterometer, SAR) instruments are unable to retrieve reliable wind speeds significantly above 25 m/s mostly due to signal saturation. Satellite measurements of high wind speeds derived from current and historical passive microwave radiometers are often hampered by heavy rain impacts. A new generation of spaceborne low microwave frequency radiometers operating at L-band (~1.4 GHz) (SMOS, AQUARIUS and SMAP) and dual C-band (AMSR-2) are now able to retrieve estimates of extreme surface wind speed over the ocean within wide swaths (>1000km) coverage, a spatial resolution of ~40 km and revisit of ~3 days for an individual satellite. L-band measurements are almost unaffected by rain and atmospheric effects, while dual C-band data offer efficient means to strongly minimize these impacts. Over the ocean surface, foam coverage is enhanced at wind speeds >~10 m/s. Wind and wave generate foam which modifies the surface emissivity and in turn the brightness temperature (Tb) measurements over a stormy ocean. New geophysical model functions have been derived to retrieve reliable ocean surface wind speeds from Tb variations over Tropical Cyclones that have been validated using aircraft measurements (Reul et al., 2016). Combined L- and dual C-band satellite instruments are now probing storm surface wind structures with an unprecedented temporal sampling to provide quantitative and complementary surface wind information of interest for operational Hurricane intensity forecasts. A database of sensor wind speed products intercepting all Tropical Cyclones during 2010-2015 has been derived.
For a brief summary of ways to access, and how to display SMOS Storm data, a quick start guide is available and can be found in the appendix section of the User Manual.
This document serves as an overview and introduction for users to SMOS-HWS products and services. For a complete discussion and access to the documentation, data products and services see http://www.smosstorm.org/Data/SMOS-STORM-Databases

Abreviations & acronyms

ADB	Actions Data Base
ADT	Advanced Dvorak Technique
AMSRE	Advanced Microwave Scanning Radiometer – E (of EoS Aqua)
AMSR2	Advanced Microwave Scanning Radiometer 2
AMSU	Advanced microwave sounding unit Radiometer onboard NOAA meteorological sat
AOML	Atlantic Oceanographic and Meteorological Laboratory
AQUARIUS	Salinity mission (of NASA/CONAE)

ASAR	Advanced Synthetic Aperture Radar (of ENVISAT)
ASCAT	Advanced SCATterometer (of MetOp)
ATBD	Algorithm Theoretical Basis Document
ATCF	NOAA Automated Tropical Cyclone Forecast system
AVHRR	Advanced Very High Resolution Radiometer
BLEND-HWS	Blended multi-mission oceanic wind speed products
CATDS	Centre d'Archivage et de Traitement des Données SMOS
CBLAST	Coupled Boundary Layer Air–Sea Transfer
CDR	Critical Design Review
CIMSS	Cooperative Institute for Meteorological Satellite Studies
CMIS	Conical Microwave Imager/Sounder
CONAE	COmision NAcional de Actividades Espaciales
DIR	Directory (of the *SMOS+ STORM Evolution project*)
DMSP	Defense Meteorological Satellite Program (of the USA)
DPM	DetailedProcessing Model
ECMWF	European Centre for Medium-Range Weather Forecast
ENVISAT	Environnent Satellite (http://envisat.esa.int)
ESA	European Space Agency
ESL	Expert Support Laboratory
EO	Earth Observation
EU	European Union
ETC	Extra-Tropical Cyclone
FR	Final Report
FROG	Foam, Rain, Oil and GPS-reflectometry
GFDL	Geophysical Fluid Dynamic Laboratory
GFS	Global Forecast System
GHRSST	GODAE High Resolution SST
GMF	Geophysical Model Function
GSFC	Goddard Space Flight Center
Hs	Significant Wave Height (also SWH)
HRD	Hurricane Research Division (of AOML)
H*WIND	NOAA National Hurricane Center Hurricane Wind Analysis products
IODD	Input/Output Data Definition
ITT	Invitation To Tender
IR	Infra Red
JMR	Jason Microwave Radiometer
JPL	Jet Propulsion Laboratory
JRA-25	Japanese 25-Year *Reanalysis* Project
JTWC	Joint Typhoon Warning Center
KO	Kick-Off
L1	Level-1
L2	Level-2
L3	Level-3
MIRAS	Microwave Imaging Radiometer by Aperture Synthesis
MR	Monthly Report
MTR	Mid-Term Review
NAH	NOAA/NWS/NCEP North Atlantic Hurricane Wind Wave forecasting system

NASA	National Aeronautics and Space Administration
NCEP	National Centers for Environmental Prediction
NDBC	National Data Buoy Center
NHC	NOAA National Hurricane Center
NOAA	National Oceanic and Atmospheric Administration
NOGAPS	U. S. Navy's Operational Global Atmospheric Prediction System
NOP	Numerical Ocean Prediction
NRCS	Normalized Radar Cross-Section
NWP	Numerical Weather Prediction
NWS	National Weather Service
OSCAT	Oceansat-2 Scatterometer
OPS	Observation Processing System (of Met Office)
OS	Ocean Salinity
PALS	Passive/Active L-band Sensor
PM	Progress meeting
PMP	Project Management Plan
PMR	Passive Microwave Radiometry
PMSL	Pressure at Mean Sea Level
PSS	Practical Salinity Scale
QC	Quality Control
RA-2	Radar Altimeter 2 (of ENVISAT)
RD	Reference Document
SAR	Synthetic Aperture RADAR
SAR	Scientific Assessment Report (of *SOS*)
SAP	Scientific Analysis Plan
SatCon	CIMSS Satellite Consensus (SatCon) product
SFMR	Step Frequency Microwave Radiometer
SIAR	Scientific and Impact Assessment Report
SLA	Sea Level Anomaly
SMOS	Soil Moisture and Ocean Salinity (mission)
SMOS-HWS	SMOS High Wind Speed products (surface wind speed and foam-related properties)
SoW	Statement of Work
SSM/I	Special Sensor Microwave Imager (of DMSP)
SSMIS	Special Sensor Microwave Imager Sounder
SST	Sea Surface Temperature
SSS	Sea Surface Salinity
STSE	Support to Science Element
TBC	To Be Confirmed
TC	Tropical Cyclone
TBD	To Be Determined
TDP	Technical Data Package
TDS	Test Data Set
TMI	TRMM Microwave Imager
TN	Technical Note (short report 10-50 pages)
TR	Technical Report (long report > 50 pages)
TRMM	Tropical Rainfall Measuring Mission
UM	User Manual

URL	Universal Resource Locator
WP	Work Package

Applicable & Reference documents

Reference	Title	Code	Date
[R.D.1]	SMOS High Wind Speed -Algorithm Theoritical Background Document- Input/Output Data Definition- Detailed Processing Model	SMOSpluSTORM_EVOLU_SHWS_ATBD_v1.1	31-05-2016
[R.D.2]	Blend High Wind Speed -Algorithm Theoritical Background Document- Input/Output Data Definition- Detailed Processing Model	SMOSpluSTORM_EVOLU_BHWS_ATBD_v1.1	31-05-2016

1-Overview of the SMOS STORM project

1.1 Scientific background

Measurements of ocean surface wind speed and wind vector fields in Tropical Cyclones (TCs) and Extra-Tropical Cyclones (ETCs) are fundamental to better forecasts of storm intensity and evolution with obvious societal benefit. Yet little progress has been made in hurricane intensity predictions compared to storm track forecasts [e.g., Harnos and Nesbitt, 2011; DeMaria et al., 2013]. This is, in part, due to limited measurements of storm intensity evolution and the structural state of the wind system in question. The latter is commonly estimated through several derived parameters, such as the Maximum Sustained Wind (MSW), defined as the 1 min average wind speed at the altitude of 10 m (e.g., at the National Hurricane Center (NHC)), the Radius of Maximum Wind (RMW), and the maximum radial extent of significant wind speed thresholds (e.g., the radial extent of 34-, 50- and 64-knot wind speed) in each geographical quadrant over the life of a tropical cyclone (Knaff et al., 2016). Better measurements of these parameters in near-real-time (NRT) lies at the heart of improved storm forecasting capability.

Although in situ measurements of MSW and important wind radii are possible using reconnaissance aircraft such as the famous NOAA Hurricane Hunters, or land/ship-based instruments, satellite data have been a major source of information due to their quasi-synoptic regular repeat coverage and global availability. The Dvorak technique is the primary satellite method for estimating MSW in TCs based on cloud pattern recognition from visible (VIS) and infrared (IR) satellite images [Dvorak, 1975; Velden et al., 2006 for a review]. There are other methods. For example, Kidder et al., [1978] relate a warm anomaly derived from satellite MicroWave (MW) brightness temperature oxygen band (~55 GHz) to the hurricane pressure gradient. The Dvorak Technique continues to be the standard and most-successful method for estimating TC intensity where aircraft reconnaissance is not available (all tropical regions outside the North Atlantic and Caribbean Sea) although it has known limitations and flaws (see Velden et al., 2006 for a review). In particular, MSW

estimates from methods that rely on VIS, MW (at frequency > 50 GHz) and IR observations of the upper atmospheric levels of TCs are uncertain because the ubiquitous cirrus canopy of hurricanes is opaque in those wavelengths. Assumptions on the local vertical structure of the atmospheric boundary layer and drag coefficient are required to infer the MSW at a height of 10 m above the sea surface from these cloud-top observations (eg. Dunion et al. 2002; Dunion and Velden 2002). Complementary measurements from other techniques, allowing more 'direct' sensing at surface level such as cloud-penetrating radar scatterometery, synthetic aperture radar (SAR) and microwave frequency radiometers, operating in the 1 to 11 GHz frequency bands (L- to X-bands) have been critical.

Real and synthetic aperture C-band radars (4-7 GHz), such as the Advanced SCATterometer (ASCAT), provide accurate estimates (<2 m s−1) of the 10 m height wind velocity below ∼25 m s−1 based on a complex geophysical model function driven by measurements of the normalized radar cross section (σo) obtained at different azimuth angles (e.g., Quilfen et al., 1998). Such data are especially helpful in identifying incipient tropical cyclones and the extent of tropical storm force (17 m s−1 ∼34 kt) wind speeds. C-band radar measurements are less prone to rain contamination than higher frequency systems but they still suffer heavily from rain contamination in TC's eye wall and outer rain band regions where intense rain fall strongly impacts microwave radiation (Weissman et al., 2002; Meissner and Wentz, 2009 Brennan et al. 2009). More importantly, it is well known that σo in HH or VV polarization is susceptible to signal saturation (e.g., Donelly et al., 1999, Fernandez et al. 2006) at about ∼25-30 m s−1 (Powell et al. 2003; Donelan et al., 2004). However, recent experimental evidence using the Imaging Wind and Rain Airborne Profiler (IWRAP, Sapp et al, 2013) aircraft radar system configured in cross-polarized (VH) mode, showed no evidence of saturation up to wind speeds of 60 m s−1. Unfortunately there are currently no satellite scatterometer systems designed to acquire VH measurements. Recent methods involving cross-polarized C-band SAR data also show better capabilities than dual-polarization alone to retrieve TC wind speed (Zhang and Perrie, 2012; Horstmann et al., 2013). Despite these current drawbacks, scatterometery remains a fundamental data set for wind speed determination over the ocean surface.

In recent years, microwave radiometry has played an increasing role in TC measurements pioneered by the successful development and application of the Step Frequency Microwave Radiometer (SFMR) onboard the National Oceanic and Atmospheric Administration (NOAA) and Air Force reconnaissance aircraft (Uhlhorn et al., 2007). It is well known that the microwave brightness temperature of the ocean is strongly dependent on variations in surface emissivity associated with increasing foam coverage due to whitecap and streaks induced by wave breaking, wind shear of the wave crest (Holthuijsen et al., 2012; Norberg et al., 1971, Ross and Cardone, 1974, Webster et al, 1976) and the distribution of foam formation and sea-spray layer thicknesses (Anguelova and Gaiser, 2012; Camps et al., 2005; Reul & Chapron, 2003, Raizer). The continuously increasing "whitening" of the sea surface as the wind speed intensifies above ∼10-12 m s−1 reaches an almost fully foam-covered ocean 'surface' in the most intense hurricane force situations. This induces a corresponding continuous growth of the radio-brightness emission from the sea surface, as observed by a low-frequency microwave radiometer. Provided atmospheric (rain, cloud liquid water, vapor, oxygen, etc…) and sea-spray droplets contributions can be well accounted for, the measured radio-brightness contrast change can be related to surface wind speed and/or sea state.

Until very recently, multi-frequency (∼6.9 - >89GHz) satellite microwave radiometers (e.g., SSM/I, SSMIS, TMI, TRMM, AMSR, AMSU, CMIS, AMSR-E, and WindSAT) all

operated at frequencies higher, or equal to C-band, and, if available, only acquired data from one single C-band channel. These satellite instruments are very efficient tools to infer cloud liquid water, water vapor, wind speed, rain rate, and, sea surface temperature (SST) in certain conditions typically below hurricane force winds. However at these frequencies, atmospheric absorption, emission and scattering associated with high cloud liquid water content and precipitation prevalent in cyclones can have a large impact on brightness temperatures. Consequently, it is challenging to obtain accurate ocean surface wind and whitecap properties beneath tropical cyclones at these frequencies. The measurement of ocean surface wind speeds during precipitation events has been a long-standing problem for satellite passive microwave radiometers. Algorithms have been developed that are able to measure ocean surface wind speeds with an accuracy of ∼2 m s−1, in rain free conditions [Bettenhausen et al., 2006]. Unfortunately, these algorithms break down completely as soon as light rain is present. For accurate retrievals of wind speeds when precipitation in present it is essential to use different frequencies, whose spectral signature make it possible to find channel combinations that yield brightness temperature with sufficient sensitive to wind speed and low sensitivity to rain [Yueh, 2008; Meissner and Wentz, 2009; El-Nimri et al., 2010]. This principle led to the development of the SFMR instrument, which measures the brightness temperature of the ocean surface using six distinct C-band frequencies, including frequencies which permit the measurement, and correction for, both atmospheric effects (mostly rain) and retrieve surface wind speed. Unfortunately, the SFMR is limited by aircraft range in the North Atlantic and Eastern Pacific, and there is still no equivalent sensor capability flying in space today.

Today most available active and passive orbiting sensors operating in the low microwave frequency bands still show limited performance when retrieving surface wind speed estimates above tropical storm force (Powell, 2010). For passive sensors, this is largely because of the difficulty to precisely separate wind from rain and other atmospheric effects, and for active sensors, it is because of σo saturation above hurricane force.
A new generation of microwave satellite sensors, namely the ESA Soil Moisture and Ocean Salinity (SMOS), the NASA Soil Moisture Active Passive (SMAP), and the JAXA Advanced Microwave Scanning Radiometer 2 (AMSR-2) missions, provide enhanced and complementary surface wind speed sensing capabilities in extreme tropical cyclone conditions. They operate either at a significantly lower microwave frequency than their predecessors: this is the case for SMOS and SMAP which operate at 1.4 GHz (L-band), or are equipped with dual-frequency C-band channels (AMSR-2).

In the frame of the SMOS storm project, we have been generating retrieved winds from SMOS, AMSR-2 and SMAP data from 2010 to 2016 with a temporal coverage depending on the mission lifetime. The database of these wind products organised in swath format (so-called level 2) or daily (level3) that were generated from AMSR-2 will be described in this document.

Measuring High Wind Speed with SMOS and SMAP L-band radiometers

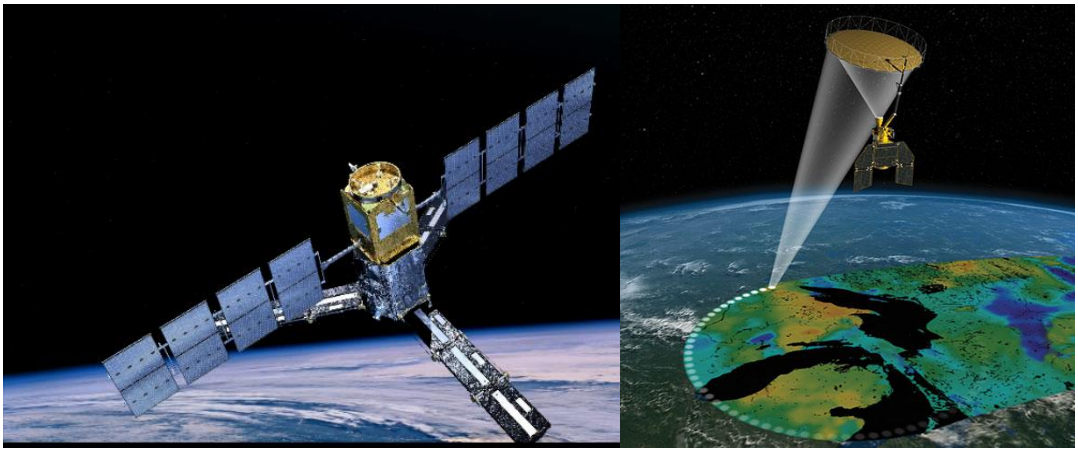

Figure 1: Artistic views of the ESA SMOS (left) and NASA SMAP (right) satellite missions.

SMOS (Kerr et al., 2010) and SMAP (Entekhabi et al., 2014) radiometers (see Figure 1) both operate at L-band (~1.4 GHz, 21 cm wavelength), a protected frequency primarily chosen to allow global measurements of soil moisture and ocean surface salinity from space (Mecklenburg et al., 2016). SMOS and SMAP were launched late 2009 and early 2015, respectively. Both sensors provide L-band brightness temperature imaging of the Earth over a ~1000 km wide swath at about ~40 km nominal resolution, and with global coverage in about 3 days. SMOS is a fully-polarized interferometric radiometer and acquires multi-incidence angle (0°-60°) images of an Earth target. SMAP sensor is a real aperture radiometer and probes the Earth brightness at a fixed incidence angle of ~40°, at two opposite azimuthal directions (fore and aft views).

It was first demonstrated (Reul et al., 2012, Reul et al., 2016) that SMOS passive measurements offer new and unique opportunities to complement existing ocean satellite high wind observations in TCs and severe weather. Upwelling radiation at 1.4 GHz is indeed significantly less affected by rain and atmospheric effects than at higher microwave frequencies. In particular, the absorption due to rain of upwelling radiations is two orders of magnitude larger at C-band frequencies than at L-band (see Figure 2 in Reul et al., 2012). In Reul et al. (2016), the SMOS measured L-band storm-induced microwave brightness temperature excess has been related to surface wind speed. Using a large ensemble of co-located SFMR aircraft winds (Uhlhorn et al., 2007), and H*WIND analyses (Powell et al., 1998), collected for an ensemble of storms between 2010 and 2015, the inferred Geophysical Model Function (GMF) is a quadratic relationship of the surface wind speed at a height of 10m (U10). Validation of the inferred surface wind speed products shows that surface wind speed can effectively be retrieved from SMOS data using this GMF with an RMS error on the order of 5 m s-1 (~10 kt) up to ~50 m s-1 (~100 kt). Similar results involving SMAP data and a slightly different GMF were recently reported by Yueh et al. (2016a).

Uncertainty in the SMOS retrieved wind speed must be minimized from an ensemble of instrumental and geophysical issues. These include radiometric uncertainties: badly corrected residual solar effects on the brightness temperature images, varying noise level depending on the pixel location within the field of view, and, brightness temperature image reconstruction biases (e.g., seasonal, orbital, at land/sea transitions, …). Most troublesome is the fact that, although the SMOS radiometer frequency of 1.413 GHz belongs to a frequency band (1400-1427 MHz) protected by international regulations, contamination by unwanted out-of band emissions from poorly maintained transmitters and possibly illegally operating

emitters (radars, telecommunication, …) compromise the quality of the SMOS retrievals in some areas (Oliva et al., 2016). A high number of radio-frequency interference (RFI) events are observed worldwide, and particularly impact the quality of the SMOS retrieved winds along the coasts of Asia. As SMOS, launched in 2009, was the first satellite to operate in L-band, it does not have any on-board hardware/software to filter RFI. This issue is significantly less important for SMAP, as it is equipped with on-board frequency/time-domain-based RFI filters. Finally, some geophysical contributions to the observed brightness signal at L-band in stormy conditions are poorly known and/or accounted for in the retrieval algorithms. These include uncertainties on the sea surface salinity at targets located in highly dynamical and variable areas (such as the Amazon, or, Mississippi river plumes), inaccuracies in the sea surface temperature retrieved from MW observations under heavy precipitations (Wentz et al., 2000), the potential impact of intense rain and ice clouds (while much weaker than at C-band, Reul et al., 2016 identified a potential effect of intense rain and ice clouds on SMOS L-band data).
Further, from a strict sensor physics point of view, L-band radiometers do not directly measure surface winds. Radio-brightness sensitivity is mostly controlled by foam formation structure changes at the ocean surface under wind-wave forcing conditions. The respective contributions of wind and waves to the measured excess brightness signal stay poorly known. Variations in sea states possibly found for a fixed radial wind speed in the different storm quadrants (Kudryavtsev et al., 2015) likely contributes to uncertainties on the retrieved surface winds (Ulhorn et al., 2007).
Despite these challenges, extremely lucrative estimates of the surface wind speeds at and above hurricane force conditions (> 33 m/s) are readily obtained using L-band storm-induced microwave brightness temperature excesses.

Measuring High Wind Speeds with the dual C-band channels of AMSR2

Figure 2: Artistic JAXA AMSR-2 satellite mission.

To properly evaluate and possibly compensate for precipitation and other atmospheric contributions to the brightness changes observed by C-band radiometers in TCs, the wind speed retrieval algorithm requires measurements from several C- or X-band frequency channels. Small changes in the respective contribution of wind and rain to the signal measured by each channel can then be used to accurately infer both quantities (Uhlhorn, 2014). Radiometers equipped with frequency channels that are far from each other (e.g., C-band and Ku-band) are more complex. With significant differences in footprint dimensions and, consequently, different beam filling effects, it is difficult to precisely separate the contribution from precipitation and atmospheric sources.
The Advanced Microwave Scanning Radiometer (AMSR and AMSR-R) sensor only operated a single ~6.9 GHz channel (V and H polarization) and had limited capacity in this respect. The follow-on, AMSR2, on board the GCOM-W satellite launched in May of 2012, has C-band channels at frequencies 6.925 and 7.3 GHz (Imaoka et al., 2010). This instrument features a 1450 km-wide swath, an improved calibration with respect to AMSR-E, and a higher spatial resolution (35 km x 62 km for the C-band channels) due to larger antenna diameter. The addition of the two new C-band channels was initially intended for RFI identification, but they can be exploited in to retrieve surface wind estimates. Signals at these two C-band frequencies have similar sensitivity to the sea wind speed, but differ in sensitivity to rain by about 12%. An efficient multi-frequency retrieval algorithm developed in a series of papers by Zabolotskikh et al. (2013, 2014, 2015, 2016) demonstrate significant success when retrieving sea surface wind speed and rain in both tropical cyclones and polar lows. Accuracy of the AMSR2 retrieved wind speed in storms is comparable to the one obtained from SMOS and SMAP L-band sensors in the range 34-100 kt, i.e. ~10-12 kt (see, Zabolotskikh et al., 2014).

1.2 Overview of the SMOS STORM BHWS processing

In the present document, we will describe the algorithm we used to generate surface wind speed blend products from individual HWS products.

The main choice was to use an optical flow deformation field, combined with cyclone trajectories when available, to morph any satellite high wind speed observation to the Blend analysis time. Following the space time evolution of surface wind speed (Figure 1) is allowing to combine more observations than usually possible with simple collocation techniques limited to smaller time windows (typically 6 hours). However, allowing for a larger observational window also implies some significant time evolution from observation to analysis time and some wind speed time evolution is also estimated to produce a more reliable blend wind product. Validation of this algorithm has started using both a direct collocation between morphed observations from a given satellite measurement to another independent one and indirectly evaluating the blend wind speed on the Sea Surface Salinity retrieval process. The details of this validation will be provided in a separate BLEND-HWS wind product validation report.

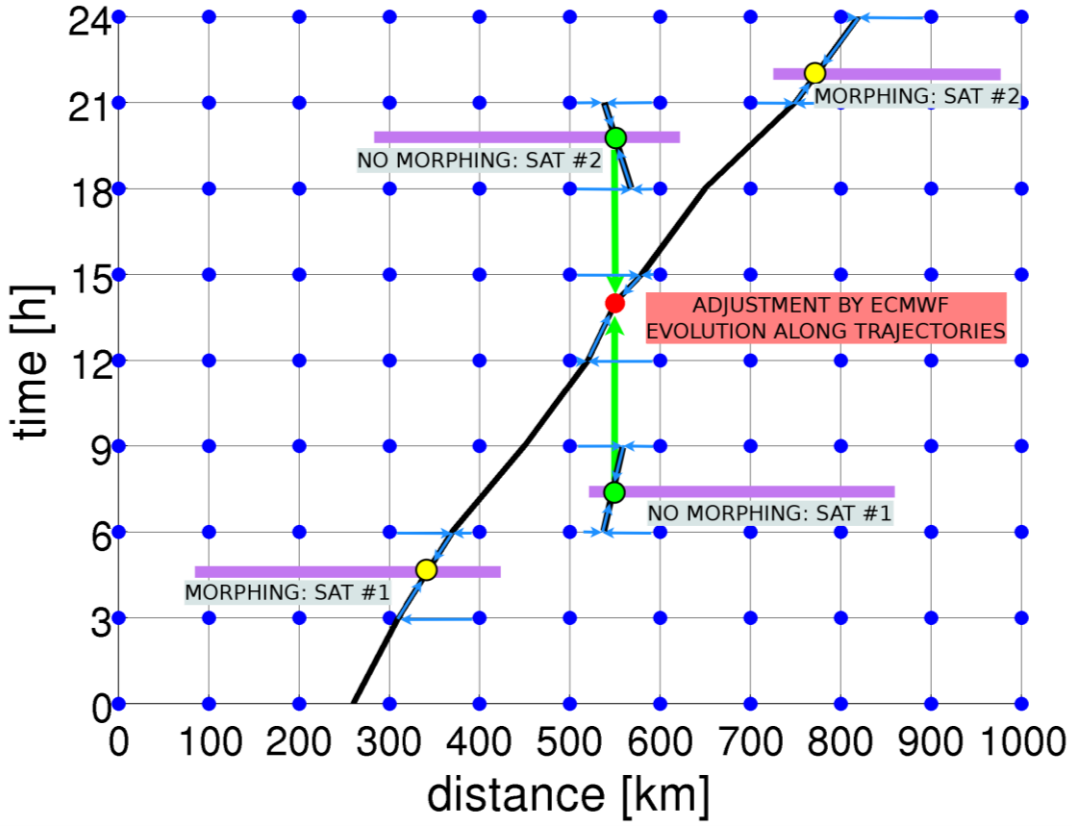

Figure 1 : Space time diagram, showing ECMWF wind (blue dots), satellite observations (magenta lines) and interpolations using morphing from optical flow trajectories (black) or simple collocation with no morphing (green).

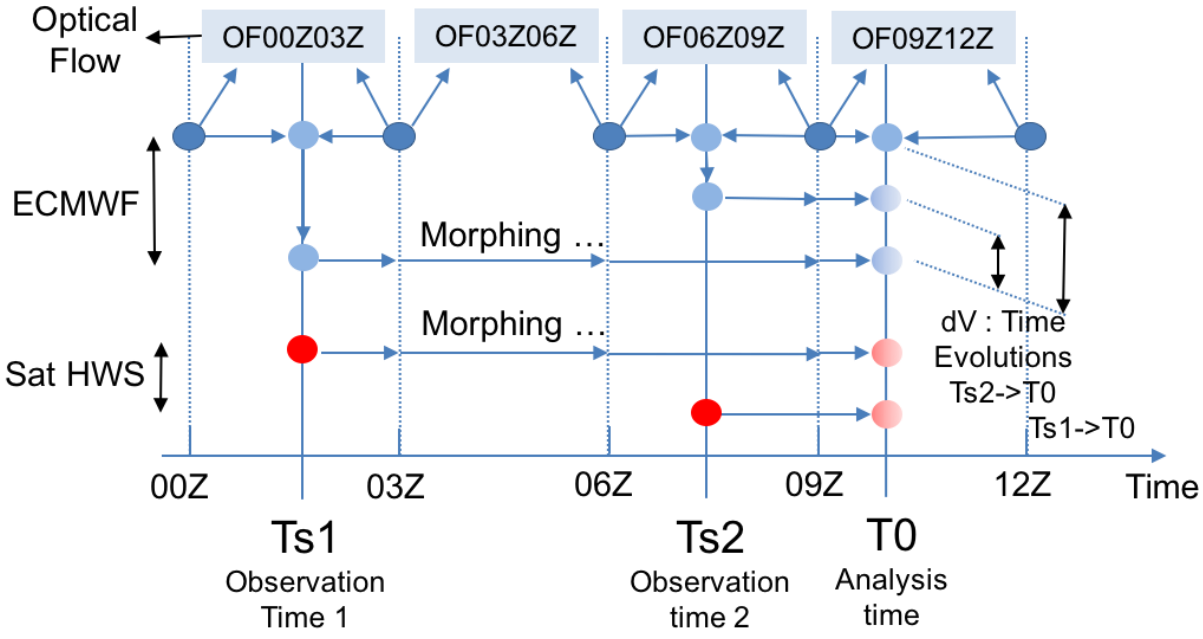

Figure 2: Schematic view of the Lagrangian interpolation processing timeline.

A general overview of the main algorithm steps is given in Figure 2. Having selected the HWS products at different time Ts we want to process, within +-12hours from Blend wind analysis time T0, we then apply a series of processing steps, namely :

- **Step 1 :** From ECMWF model 3 hourly outputs and best track cyclone trajectories (ibtracs v03r09) compute 3 hourly merged deformation fields (OF00Z03Z, …)
- **Step 2 :** Setting a blend wind analysis time T0 and surrounding observation time windows [T0,T0+k], k from -12h to +12h.
- **Step 3 :** Lagrangian interpolation of ECMWF model 3 hourly outputs to the center time Ts of each observation windows using merged deformation field.
- **Step 4 :** Morphing of a regular grid (analysis grid) from analysis time T0 to the center time Ts of each observation time windows.
- **Step 5 :** Lagrangian interpolation of each HWS observations and colocated interpolated ECMWF field falling in any of the observation time windows (less than 12 h from analysis time) at the position of morphed analysis grid (cf along black trajectory on Figure 1)

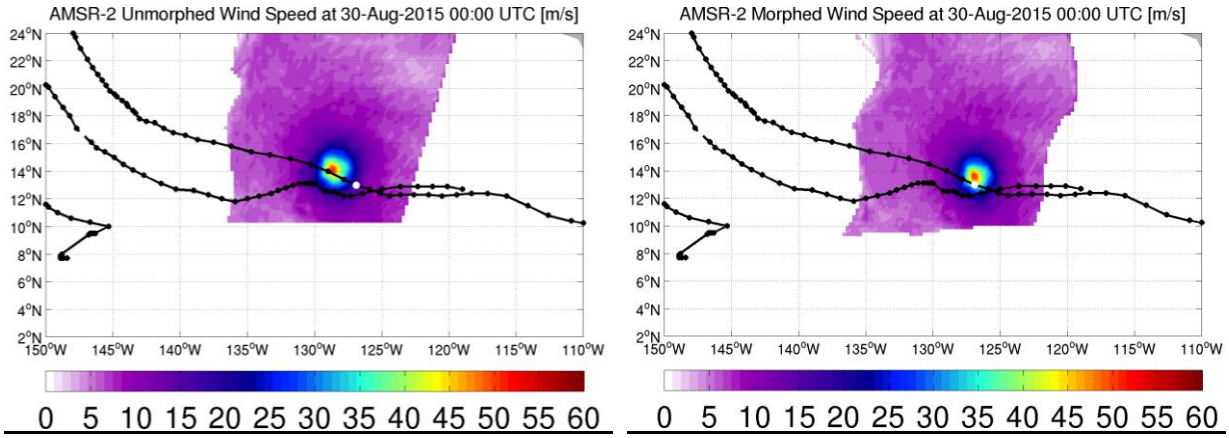

Figure 2 : HWS field before (left) and after (right) morphing to analysis time. White dot is the best track storm center at analysis time.

- **Step 6 :** Langrangian interpolation of ECMWF model to analysis time T0.
- **Step 7 :** Estimation of ECMWF wind speed time evolution from Ts to T0 as the difference between ECMWF wind speed at Ts morphed to T0 and ECMWF wind speed interpolated at T0.
- **Step 8 :** Estimation of HWS at T0 for each satellite observations from the sum of morphed satellite HWS at T0 + ECMWF wind speed time evolution from Ts to T0.
- **Step 9 :** Estimation of a blend product as the mean and variance of HWS at T0 from each HWS brought to analysis time.
- **Step 10 :** Output netcdf file.

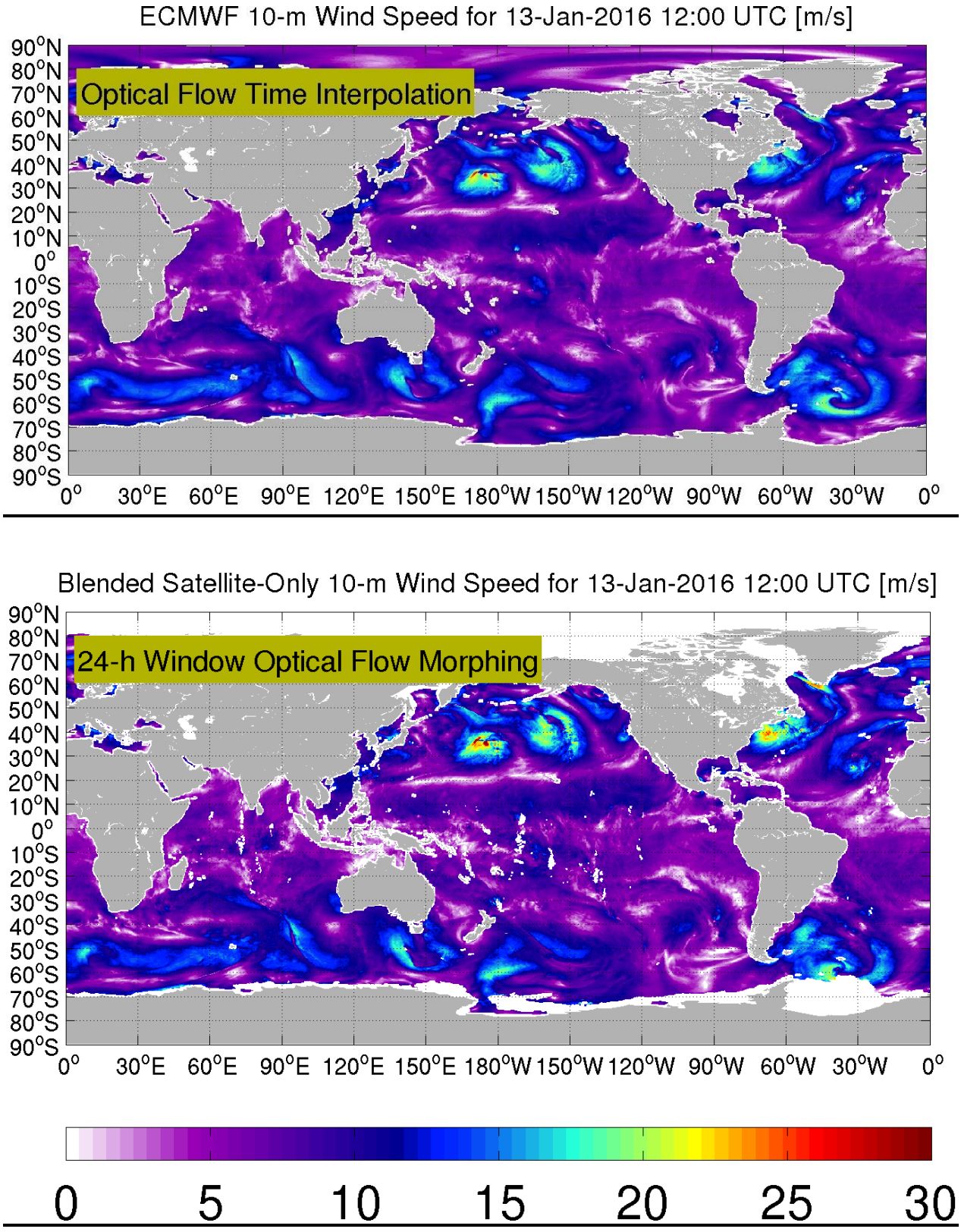

Figure 3 : Wind speed fields at analysis time Jan 13 2016 at 12:00 UTC from morphed ECMWF wind speed at observation time (upper pannel) and all morphed HWS from observations less than 12h from analysis time (lower pannel)

3-SMOS STORM BHWS Data products

The SMOS STORM BHWS database is composed of hourly merged gridded wind speed data (Level 4) from SMOS/AMSR-2 and all other satellite wind sensors. All files for these sensors are provided in netcdf format.

3.1 Database Space-Time Coverage

Level 4 blended wind speed data are global. The database cover the time-period :

- from 1st January 2015 at 00:00 to 31 December 2015 at 23:00
- from 22nd August 2016 at 00:00 to 9 September 2016 at 23:00
- from 1st January 2017 at 00:00 to 18 February 2017 at 23:00

3.2 Level 4 BLEND HWS files in Netcdf format

Each Level 4 BLEND HWS product include the merged wind speed data given on a regular 0.25° x 0.25° resolution grid.

The generic filename convention for the BLEND High Wind Speed products is:

blended_winds.YYYYMMDD.HHMMSS.blend.nc

The date: ***YYYYMMDD.HHMMSS*** indicates the analysis time (year-month-day hour minute seconds)

Each file for each analysis time includes each invidual observations morphed to analysis time as well as the blend mean and variance together with an ensemble of variables descrived in the table 3 below :

Dimension name	Description
latitude	Latitude of blend product
longitude	Latitude of blend product
sensor	Sensors used in the blend product
time	Analysis time
name	The name of wind sensor in ascii (max 7 chars)
source	The wind speed processor used, in ascii (max 100 chars)

Variable name	Description	Unit	Dimension	Precis
latitude	Latitude of blend product	Deg N	lat	float
longitude	Latitude of blend product	Deg E	lon	float
time	Blend HWS analysis Time	Time (ISO)	1	float
cyclone_weight	weight applied to cyclone track (ibtracs v03r09) for morphing	N/A	Lon,lat	float

ws10_ecmwf_anal	ECMWF 10-m wind speed interpolated to analysis time	m/s	Lon,lat	float
ws10_mean	blended wind speed (mean over retrievals)	m/s	Lon,lat	float
ws10_count	number of retrievals used to compute the mean wind speed		Lon,lat	int
ws10_stdev	standard deviation over retrievals used to compute the mean wind speed	m/s	Lon,lat	float
ws10_hw_flag	1=mean include only L-band and AMSR-2 wind speeds; 0=mean includes all wind speeds except those derived from L-band instruments and AMSR-2	N/A	Lon,lat	byte

Sensor names	Sensor sources
smos	IFREMER L-Band high wind speed model function
smap	IFREMER L-Band high wind speed model function applied to SMAP data from ftp://n5eil01u.ecs.nsidc.org
amsr2hw	Remote Sensing Systems AMSR2 daily product version 7.2
wsat	Remote Sensing Systems WindSat daily product version 7.0.1
gmi	Remote Sensing Systems GMI daily product version 8.1
ssmi16	Remote Sensing Systems SSM/I 16 daily product version 7
ssmi17	Remote Sensing Systems SSM/I 17 daily product version 7
metopa	Remote Sensing Systems METOP-A daily product version 2.1
rs	Remote Sensing Systems Rapidscat 12.5km Slice Composites Level 2B (NSCAT 2014 algorithm)

An Example content of a netcdf file :

```
netcdf blended_winds.20170218.000000.blend {
dimensions:
        latitude = 721 ;
        longitude = 1441 ;
        sensor = 9 ;
        pass_direction = 2 ;
        time = 1 ;
        name = 7 ;
        source = 100 ;
variables:
        float latitude(latitude) ;
                latitude:units = "degrees_north" ;
        float longitude(longitude) ;
                longitude:units = "degrees_east" ;
```

```
        float time(time) ;
                time:units = "days since 1990-01-01 00:00:00 UTC" ;
        float cyclone_weight(longitude, latitude) ;
                cyclone_weight:units = "nondimensional with range [0,1]" ;
                cyclone_weight:description = "weight applied to cyclone track (ibtracs
v03r09) for morphing" ;
        float ws10_ecmwf_anal(longitude, latitude) ;
                ws10_ecmwf_anal:units = "m/s" ;
                ws10_ecmwf_anal:description = "ECMWF 10-m wind speed interpolated to
analysis time" ;
                ws10_ecmwf_anal:_FillValue = -32768.f ;
        float ws10_mean(longitude, latitude) ;
                ws10_mean:units = "m/s" ;
                ws10_mean:description = "blended wind speed (mean over retrievals)" ;
        int ws10_count(longitude, latitude) ;
                ws10_count:description = "number of retrievals used to compute the mean
wind speed" ;
        float ws10_stdev(longitude, latitude) ;
                ws10_stdev:units = "m/s" ;
                ws10_stdev:description = "standard deviation over retrievals used to
compute the mean wind speed" ;
        byte ws10_hw_flag(longitude, latitude) ;
                ws10_hw_flag:description = "1=mean include only L-band and AMSR-2 wind
speeds; 0=mean includes all wind speeds except those derived from L-band instruments
and AMSR-2" ;
        char sensor_names(sensor, name) ;
        char sensor_sources(sensor, source) ;

// global attributes:
                :analysis_time_utc = "18-Feb-2017" ;
}
```

4- SMOS STORM Data Access and Discovery

The BHWS datasets produced by the SMOS+Storm project include:

- Level 4 datasets : blended wind speed obervations (2015-2016-2017), one file every hour (see dedicated User Manuel)

All these data are available through FTP at :
ftp://eftp.ifremer.fr/storm/data/smosstorm/l4/blended/

To connect, go to http://www.smosstorm.org/Data then you first need to get an account: please fill in this short form and you will get immediate access credentials. Then go to ftp://eftp.ifremer.fr and log in with the identifier and password provided to you. Go to smos/smosstorm repository and you will see the forementioned datasets.

The SMOS+Storm atlas is also accessible with the following image browser, including access links to the data in Netcdf format: http://www.ifremer.fr/cersat/images/smosstorm2/

For any access issue, please contact CERSAT help desk (cersat@ifremer.fr).